Validation and Refinement of the MODIS Land-Surface Temperature Product

Zhengming Wan

ERI, University of California, Santa Barbara, CA 93106, USA

Basic Considerations in MODIS LST Algorithms (I)

1. LST is retrieved from TIR data only in clear-sky conditions.
   LST is not mixed with cloud-top temperature in the atmospheric product (TIR signal from surface cannot penetrate clouds to reach satellites).
2. LST is defined by the radiation emitted by the land surface observed by MODIS at the instantaneous viewing angle.
   Applications may need LST at different angles (nadir or 50^o from nadir).
3. Proper resolving of the land-atmosphere coupling is the key in retrieving surface & atmospheric properties.

   Integrated retrieval is possible but it takes a lot of computing time.

   Use multi-bands in the atmospheric windows for the LST retrieval.

   The values of atmospheric temperature and water vapor are useful to improve the LST retrieval. However, there may be large errors in these values. Use them as indicates of ranges or initial guesses only.

4. Input data: MOD021KM, MOD03, MOD07, MOD10, MOD12, MOD35 & MOD43.

Basic Considerations in MODIS LST Algorithms (II)

5. The standard MODIS cloudmask product (MOD35 and MYD35) is used because it is one of the best cloudmask products available and it is good in most cases. However, mismasking (cloudy pixels as clear-sky pixels at 99% confidence, or clear pixels at 99% confidence as uncertainly clear) exist in all coudmask products. Therefore, it is important to properly use this cloudmask product and remove LSTs under effects of cloud contaminations after the initial LST generation in the production system.

6. The split-window LST algorithm is the primary algorithm used to generate the MODIS LST products including the level-2 product (MOD11_L2 and MYD11_L2) and the 1km level-3 product (MOD11A1 and MYD11A1) because the surface emissivities vary within narrow ranges in the spectral ranges of MODIS bands 31 and 32 for all land-cover types but at different widths.

7. Surface emissivities do not significantly change with time because thermal infrared radiation almost does not penetrate a thin vegetation leaf (about 0.18mm thick) and its reflectance does not change with the water content in the leaf in the spectral range above 7μm, and the skin of sands and soil lands always stay in dry condition normally in clear-sky days.

MODIS LST Algorithms (I)

The generalized split-window algorithm (Wan and Dozier, 1996) in form

$$T_s = C + \left(A_1 + A_2 \frac{1-\varepsilon}{\varepsilon} + A_3 \frac{\Delta\varepsilon}{\varepsilon^2} \right) \frac{T_{11\mu} + T_{12\mu}}{2}$$

$$+ \left(B_1 + B_2 \frac{1-\varepsilon}{\varepsilon} + B_3 \frac{\Delta\varepsilon}{\varepsilon^2} \right) \frac{T_{11\mu} - T_{12\mu}}{2}$$

where $\varepsilon = 0.5\,(\varepsilon_{11\mu} + \varepsilon_{12\mu})$ and $\Delta\varepsilon = \varepsilon_{11\mu} - \varepsilon_{12\mu}$

$T_{11\mu} - T_{12\mu}$ also expressed as $T_{31} - T_{32}$ for MODIS.

- emissivities estimated from land cover types (**Snyder et al., 1998; Snyder & Wan, 1998**).

  Emissivities vary slightly even within a land cover type (crop lands may have different soils and crops in variable coverage).

  A MODIS pixel may cover several 1km grids with different land cover types.
- coefficients Ai, Bi, and C depend on viewing zenith angle (in range of 0-65°).
- coefficients also depend on ranges of the air surface temperature and column water vapor.
- only process pixels in clear-sky at different MOD35 confidences over land or in lakes.

MODIS LST Algorithms (II)

The MODIS day/night LST algorithm (Wan & Li, 1997) is performed for grids larger than MODIS pixels:

- retrieve Ts-day, Ts-night, & band emissivities simultaneously with day & night data in seven bands (bands 20, 22, 23, 29, and 31-33).
- be able to adjust the input atmospheric cwv and Ta values.
- least square-sum fitting 14 observations to solve 13 variables: Ts-day, Ts-night, cwv and Ta values for day and night, emissivities in the first six bands (small surface effect in b33) and a BRDF factor in the first three bands.
- The range of viewing zenith angle is separated into 16 sub-ranges in v5.
- Option for combined use of Terra and Aqua MODIS data in v5.
- Terrain slope is considered in v5 QA.

Radiance-based approach to valid LSTs (Wan and Li, 2008)

1. **It uses surface emissivity spectra measured or estimated, and atmospheric temperature and water vapor profiles in atmospheric radiative transfer simulations to invert the band-31 brightness temperature of MODIS observation to a LST value, and compare this value with the LST value in the MOD11 product.**
2. **This approach works because of high calibration accuracies in bands 31** & **32**.
3. **This approach has been validated by comparisons to the conventional temperature-based approach in large homogeneous fields (lakes, grassland, and rice fields) by the MODIS LST group and César Coll's group.**
4. **It is better than the conventional temperature-based approach because the large spatial variation in LSTs especially in the daytime makes it impossible to measure LSTs at 1km scale and the small horizontal variations in atmospheric temperature and water vapor profiles in clear-sky conditions support the R-based approach.**
5. **It is important to use the atmospheric profiles appropriate to the MODIS observations by constraints of time (within 2-3 hours) and distance (≤ 100km).**
6. **It is important to perform the R-based approach on a series of days and to make quality control by comparing the values of (Tb31 – Tb32) in the simulations and MODIS observations and utilizing the difference d(Tb31 – Tb32) values in QC.**
7. **The R-based approach may not work well in wet conditions or partly cloudy days because the atmospheric profiles measured by balloons may be very different from the real profiles along the paths of MODIS observations, and clouds and heavy aerosols are not included in radiative transfer simulations. For example, as surface visibility changes from 23km to 1km, Tb31 decreases by 1.5K.**

Emissivity spectra of the grassland in TX on 21 April 2005 (left) and a bare soil site near Salton Sea, CA on 21 June 2006 (right) measured by the sun-shadow method with the Bomem TIR spectroradiometer and comparisons to band emissivities in the V5 MOD11B1 product

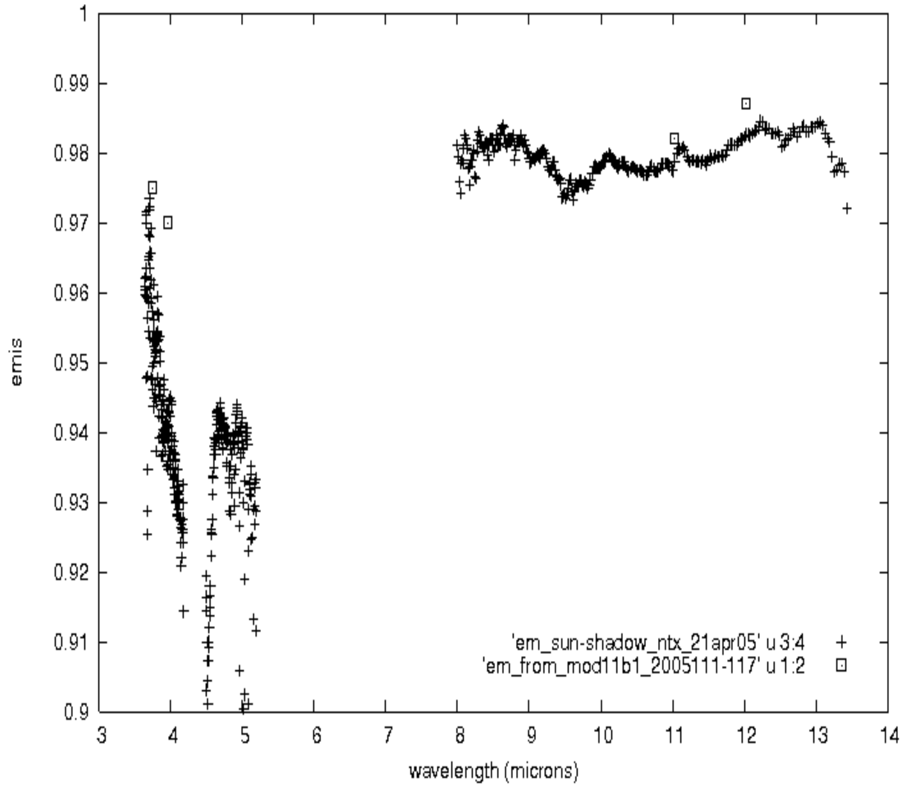

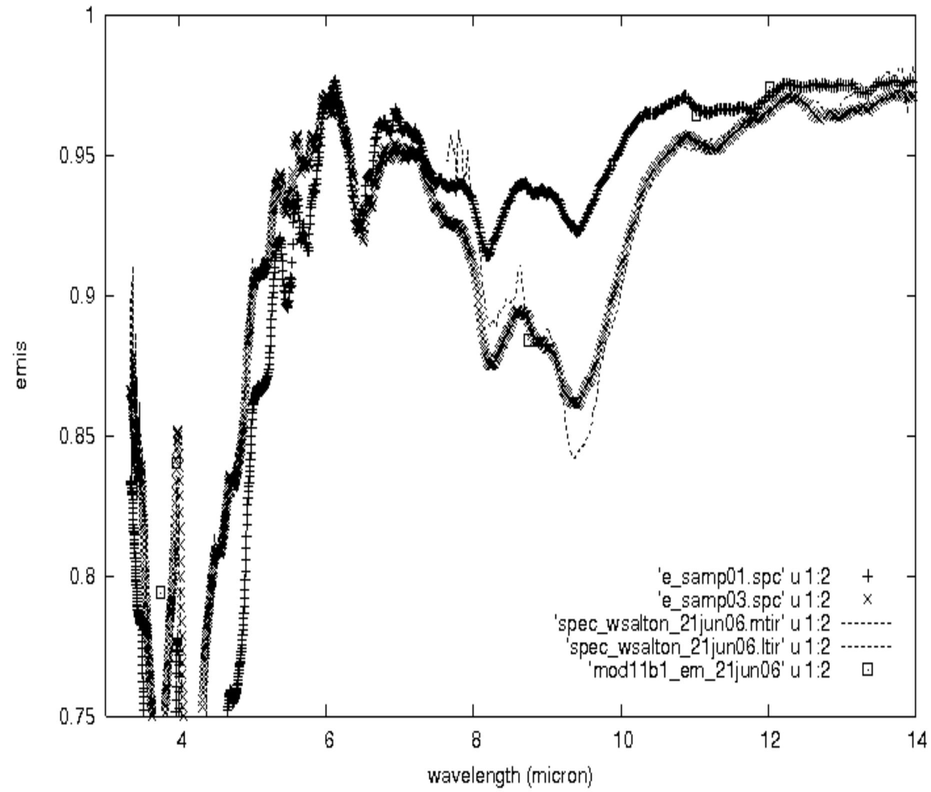

Reflectance spectra measured from sand and soil samples by the MODIS LST group. There are significant variations in the ranges of 3-5 and 8-10μm (left). The change in the reflectance/emissivity difference in bands 31 and 32 (at 11 and 12μm shown in right) may cause large errors in LSTs retrieved by the split-window algorithm.

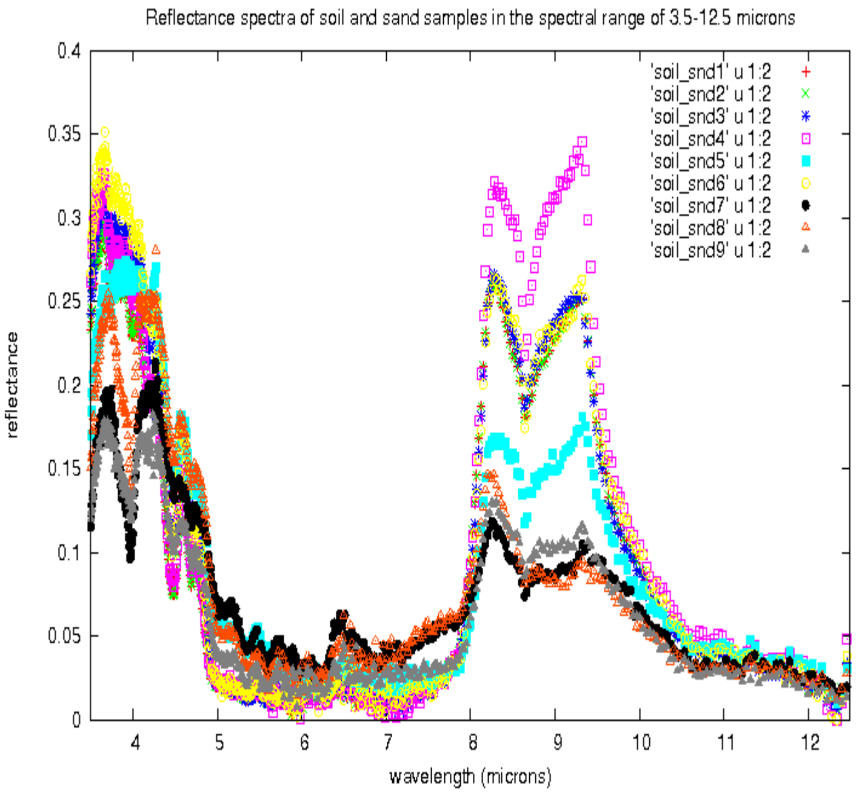

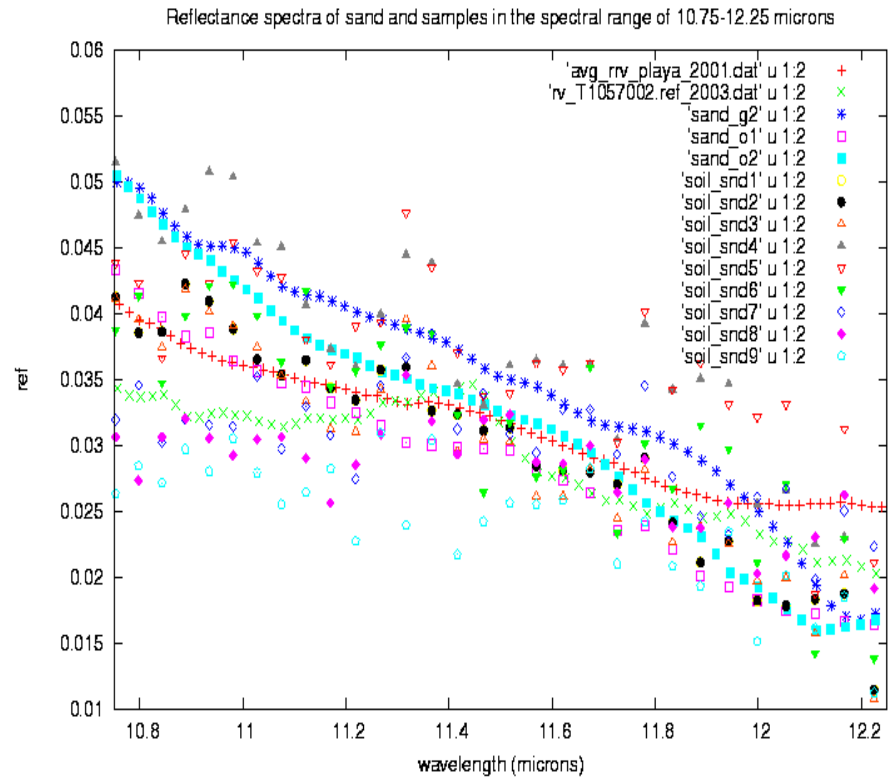

Emissivity spectra measured in laboratory from snow (left) and soil (right) samples, the spectra measured in the field at grassland and soil sites, and their combinations were used in the R-based validation of the MODIS LST products worldwide

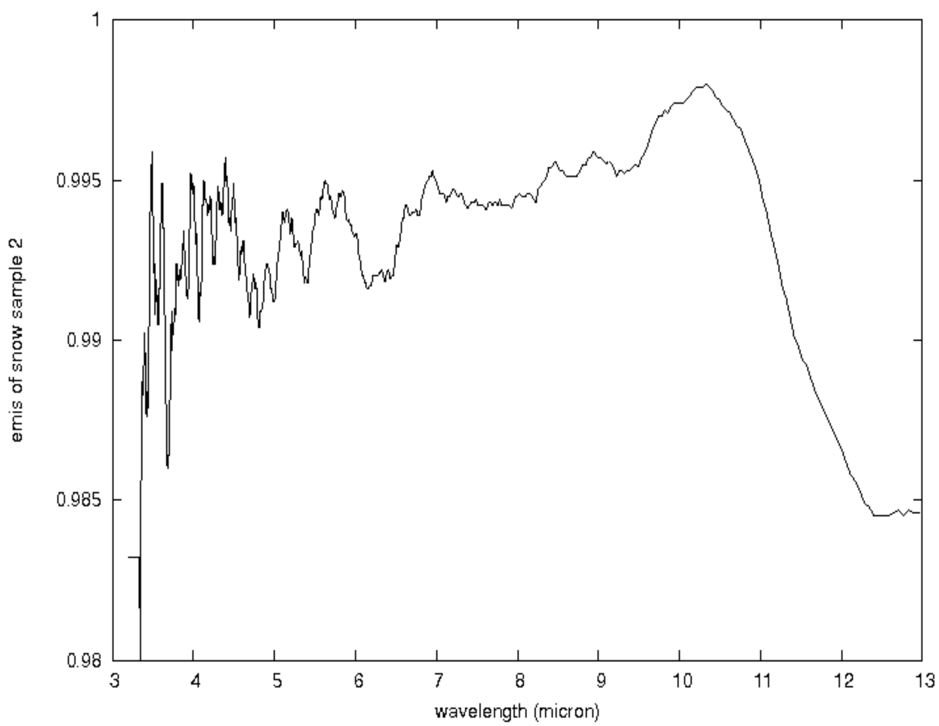

(Snow emissivity spectrum measured at Mammoth Mountain Snow Science Laboratory in 1996 http://www.icess.ucsb.edu/modis/EMIS/html/snow.html)

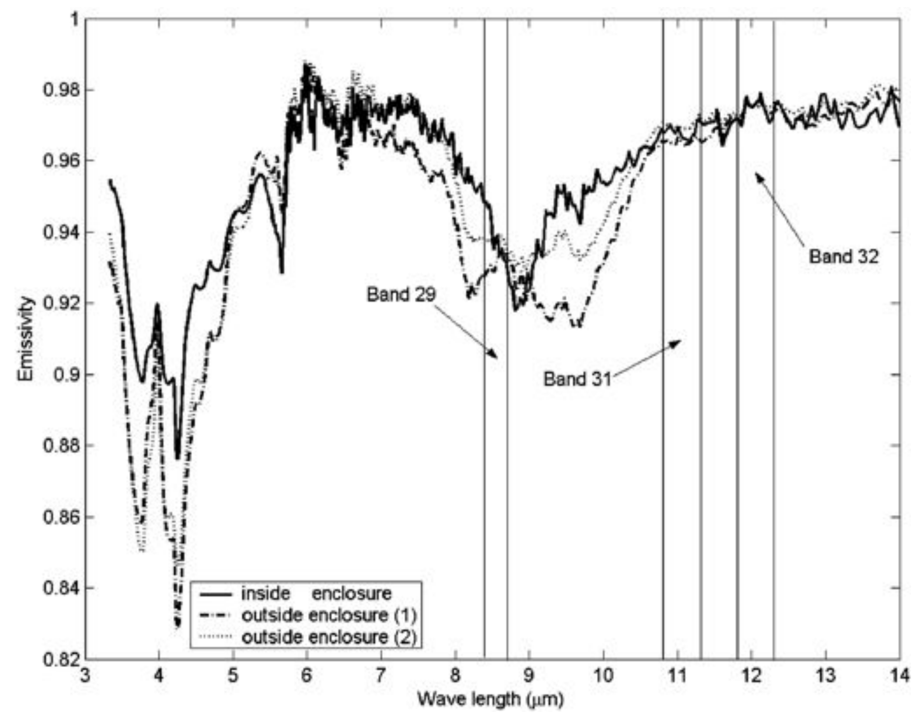

(Wang et al., Int. J. of Remote Sensing, 28: 2544-2565, 2007)

A list of the validation sites used in the past for the C5 (V5) MODIS LST products

Site	Location	Latitude, Longitude (°)	Landcover Type	Type of Validation	References
1	Lake Titicaca, Bolivia	16.247 S, 68.723 W	in-land water (0)	T-based and R-based	Wan et al (2002); Wan (2008)
2	Mono Lake, CA	38.01 N, 118.97 W	in-land water (0)	T-based	Wan et al (2002); Wan (2008)
3	Walker, NV	38.697 N, 118.708 W	in-land water (0)	T-based	Wan et al (2002); Wan (2008)
4	Salton Sea, CA	33.2 N, 115.75 W	in-land water (0)	R-based	Wan & Li (2008)
5	near Salton Sea, CA	33.25 N, 115.95 W	bare soil (16)	R-based	Wan & Li (2008)
6	Bridgeport, CA	38.22 N, 119.268 W	grassland (10)	T-based and R-based	Wan et al (2002); Wan (2008)
7	grassland, TX	36.299 N, 102.571 W	grassland (10)	R-based	Wan & Li (2008)
8	Railroad Valley, NV	34.462 N, 115.693 W	silt playa (16)	T-based and R-based	Wan et al (2002); Wan & Li (2008)
9	soybean field, Mississippi	33.083 N, 90.787 W	cropland (12)	T-based	Wan et al (2004); Wan (2008)
10	rice field, Valencia, Spain	39.265 N, 0.308 W	cropland (12)	T-based and R-based	Coll et al (2005); Wan & Li (2008)

Validation of the C5 LST Products generated in V5 tests

(at the ten validation sites)

By comparisons of LST values in the C5 MOD11_L2 and MYD11_L2 products with the in-situ values in Wan et al., 2002; Wan et al., 2004; Coll et al., 2005, and radiance-based validation results over Railroad Valley, NV in June 2003 and a grassland in northern TX in April 2005. LST errors < 1K in most cases.

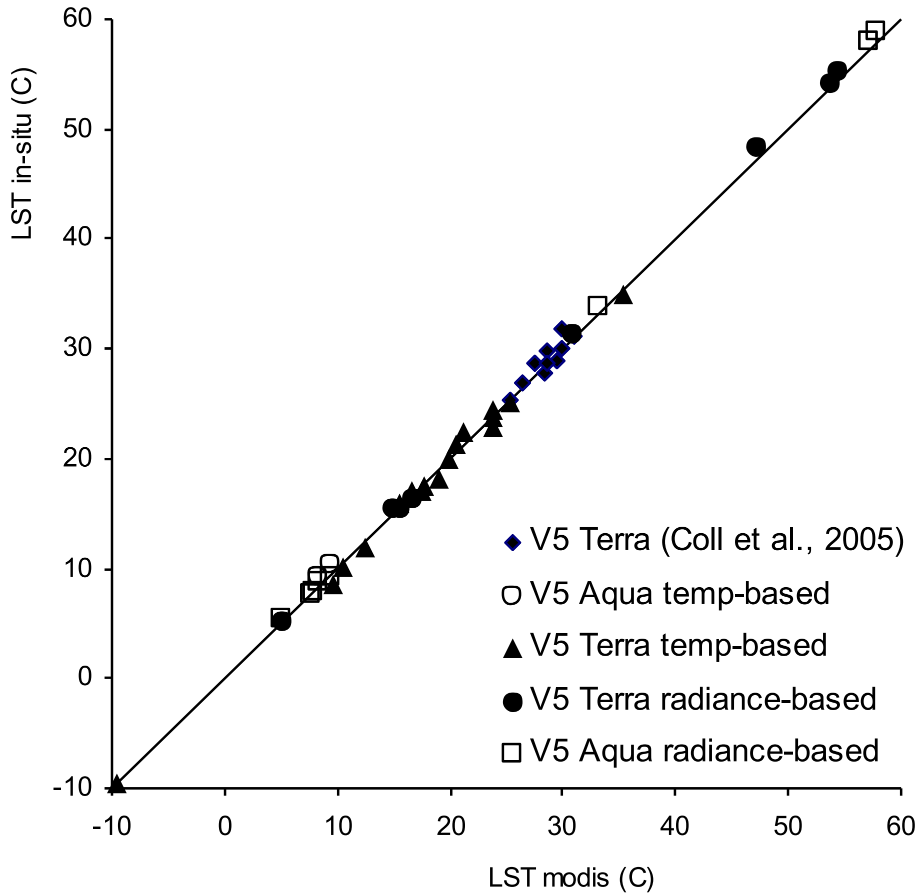

Notes for applications of C4 & C5 LST products:

- In M*D11_L2, if valid LSTs are available in both C4 & C5, their difference is less than 0.2-0.4K in most cases.

- In M*D11A1 within latitude ±28°(MODIS orbits w/o overlapping), if valid LSTs are available in both C4 & C5, their difference is less than 0.2-0.4K in most cases. Outside the latitude region, if valid LSTs are available in both C4 & C5 and at the same view time (indicating temporal average not applied in C4), their difference is less than 0.2-0.4K in most cases. Users should remove cloud-contaminated LSTs in the C4 product before using them in applications.

- LSTs severely contaminated by clouds were removed from level-3 C5 products, but not from all C4 products.
It is very difficult to remove such LSTs from the 8-day C4 M*D11A2 products because the cloud contamination effect may be reduced in the 8-day averaging.

See details in Wan (2008) and Wan and Li (2008)

The summary of R-based validation of the C5 (V5) MODIS LST products at new sites

Site	Location	Latitude, Longitude (°)	Land-cover Type (id #)	MOD11 or MYD11_L2	type of atmos. profiles	mean (std) of LST errors (K)
11	Recife, Brazil	7.96 S, 34.94 W	evergreen forest (2)	MOD11	radiosonde	0.4 (0.4)
12	Moree, Australia	29.555 S, 149.86 E	open shrubland (7)	MOD11	radiosonde	-0.8 (0.9)
13	Port Elizabath, S. Africa	33.95 S, 23.59 E	evergreen forest (2)	MYD11	radiosonde	-0.2 (0.9)
14	WLT Alert,Canada	82.4 N, 62.33 W	shrubland (7)/snow(15)	MOD11	radiosonde	0.2 (0.8)
15	South Pole	89.95 S, 0.05 E	snow/ice (15)	MOD11	radiosonde	-0.5 (0.6)
16	McMurdo,Antarctica	77.75 S, 164.1 E	snow/ice (15)	MOD11	radiosonde	0.1 (0.3)
17	Dye-2, Greenland	66.481 N, 46.28 W	snow/ice (15)	MOD11	NCEP	0.0 (0.5)
18	Summit, Greenland	72.58 N, 38.475 W	snow/ice (15)	MOD11	NCEP	0.1 (0.5)
19	Cherskij, Russia	68.75 N, 161.27 E	snow (15)/shrubland(7)	MOD11	radiosonde	0.3 (0.5)
20	Gaze, Tibet, China	32.3 N, 84.06 E	open shrubland (7)	MOD11	NCEP	-0.6 (0.2)
21	Hainich, Germany	51.079 N, 10.452 E	mixed forest (5)	MOD/MYD	radiosonde	-0.3 (0.5)
22	Paris, France	48.8 N, 2.35 E	urban (13)	MYD11	radiosonde	0.1 (0.4)
23	near Paris, France	48.45 N, 2.25 E	cropland (12)	MYD11	radiosonde	0.0 (0.6)
24	Nimes, France	43.84 N, 4.37 E	urban (13)	MYD11	radiosonde	0.1 (0.4)
25	near Nimes, France	43.828 N, 4.535 E	cropland (12)	MYD11	radiosonde	-0.1 (0.6)
26	Milan, Italy	45.485 N, 9.21 E	urban (13)	MYD11	radiosonde	-0.3 (0.7)
27	near Milan, Italy	45.297 N, 9.26 E	cropland (12)	MYD11	radiosonde	-0.3 (0.6)
28	Cuneo, Italy	44.53 N, 7.62 E	cropland (12)	MYD11	radiosonde	0.0 (0.5)
29	Payerne, Switzerland	46.855 N, 6.965 E	cropland (12)	MYD11	radiosonde	0.0 (0.5)
30	Nenjiang, China	49.07 N, 125.23 E	cropland(12)/snow(15)	MOD11	radiosonde	-0.3 (0.6)
31	Yichun, China	47.76 N, 128.88 E	mixed forest (5)	MOD11	radiosonde	0.1 (0.6)
32	Harbin, China	45.73 N, 126.65 E	urban (13)	MOD11	radiosonde	0.2 (0.8)
33	near Harbin, China	45.9 N, 127.1 E	cropland (12)	MOD11	radiosonde	0.1 (0.8)
34	Algiers, Algeria	36.72 N, 3.03 E	urban (13)	MOD11	radiosonde	-0.2 (0.9)
35	Dar-El-Beida,Algeria	36.65 N, 3.28 E	cropland (12)	MOD11	radiosonde	-0.5 (0.7)
36	Niamey, Niger	13.5 N, 2.14 E	urban (13)	MOD11	radiosonde	-0.3 (1.0)
37	Near Niamey, Niger	13.58 N, 2.07 E	grassland (10)	MOD11	radiosonde	-0.9 (1.1)
38	Tamanrasset, Algeria	22.856 N, 5.455 E	bare soil (16) in desert	MOD/MYD	radiosonde	-1.9 (1.2)
39	Bechar, Algeria	31.62 N, 2.33 W	bare soil (16) in desert	MOD/MYD	radiosonde	-1.5 (0.6)
40	Farafra, Egypt	27.04 N, 27.97 E	bare soil (16) in desert	MYD11	radiosonde	0.9 (0.4)
41	SVU, Egypt	26.285 N, 32.78 E	bare soil (16) in desert	MYD11	radiosonde	-1.6 (0.5)
42	In-salah, Algeria	27.18 N, 2.6 E	bare soil (16) in desert	MOD/MYD	radiosonde	-3.0 (0.8)

Major Problems in the V5 MODIS LST Products

1. The split-window algorithm significantly underestimates daytime LSTs when LST > Ts-air + 16K and cwv > 1.5cm (in bare soil areas) because the high LST values in these conditions were not considered in the development of the split-window algorithm. This problem can be resolved in the V6 algorithm.

2. There may be large errors in the LSTs retrieved by the split-window algorithm in desert regions because of the large uncertainties in the classification-based emissivity values. This problem cannot be resolved in the V6.

3. Because the day/night algorithm is tightly bounded with the split-window algorithm in V5, the large errors in LSTs retrieved by the split-window method in desert regions also affect the day/night algorithm. So we need to tune the day/night algorithm and make it work better even when the split-window algorithm does not work well. It is possible to make a significant improvement in the V6 day/night algorithm.

Summary for C5 MODIS LST Products

1. Daytime and nighttime LSTs in the C5 level-2 Terra & Aqua MODIS LST[1] products (M*D11_L2) retrieved by the split-window algorithm have been validated by the temperature-based approach at large homogeneous sites in lakes, rice field and dense vegetation areas. They have been also validated by the radiance-based approach worldwide at various sites including those in arid regions and cold regions. At 37 of the 42 sites, LST errors are within ±2K (±1K in most cases). Worst LST errors ranging from -2.0K to -4.5K were found at the desert site near In-salah. The LSTs at 6km grids retrieved by the V5 day/night algorithm may be validated indirectly by comparisons to the LSTs from the split-window algorithm aggregated at the 6km grids.

2. The land surface emissivities retrieved by the V5 day/night algorithm have been validated only at a few sites. Large fluctuations in the retrieved emissivities in the desert regions may be due to cloud contaminations and large errors in LSTs retrieved by the split-window algorithm.

3. Cloud contaminations and the effects of aerosols above average loadings may be a major source of errors in the MODIS LST products.
   The affected LSTs in the C5 level-2 MODIS LST products have not been removed although they were removed from the level-3 products.

New Improvements for the C6 LST Product

(1) Generate separate sets of coefficients for the viewing-angle dependent split-window algorithm over bare soil regions during daytime and nighttime. A square term of the brightness temperature difference was added to improve the accuracy slightly. The range of (LST – Ts-air) is set as from 8 – 29K for daytime LST and from -10 – 4K for nighttime LST.
This refinement significantly improved the LST retrieval, reducing the mean (std) of LST errors to -0.2 (0.5), -0.4 (0.4), -0.2 (0.4), 0.3 (0.5)K at the bare soil site west of Salton Sea and sites 38 and 39 and 41, but not so good at sites 40 and 42 where the mean (std) values are 2.8 (0.7) and -1.4 (0.6)K.

(2) Tune the day/night algorithm to improve its performance in desert regions while keeping the good V5 performance in lakes and forest/vegetation regions.

New Improvements for the C6 LST Product (cont.)

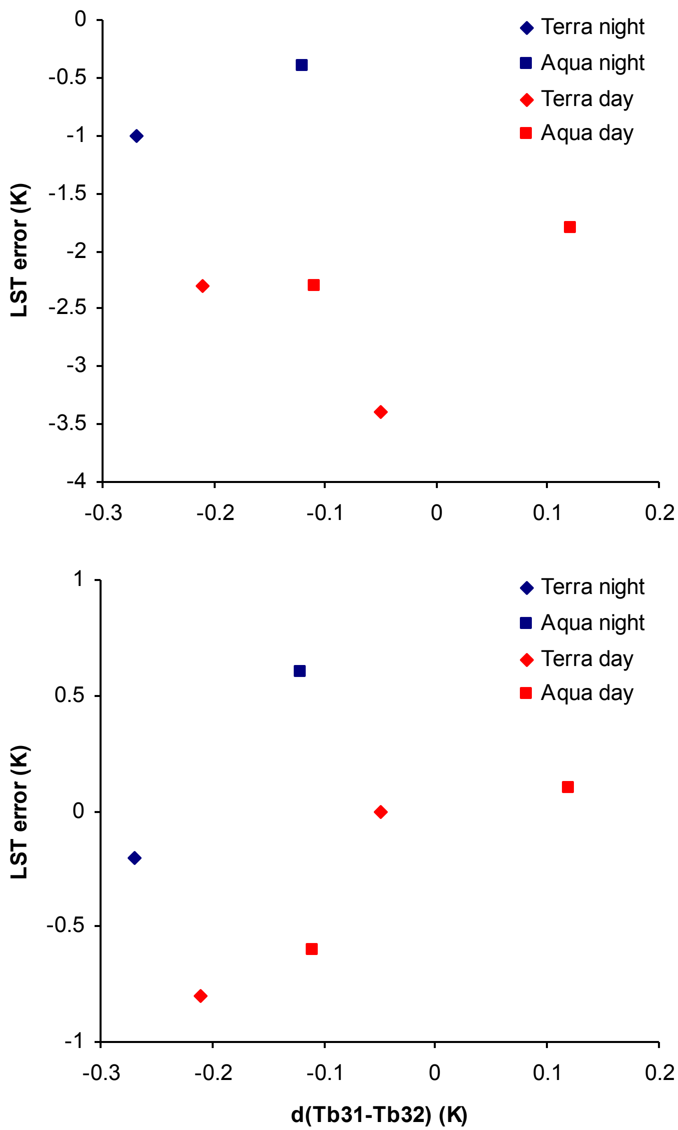

LST errors at site 5 (bare soil site west of Salton Sea) in V5 (upper) and V6 (bottom).

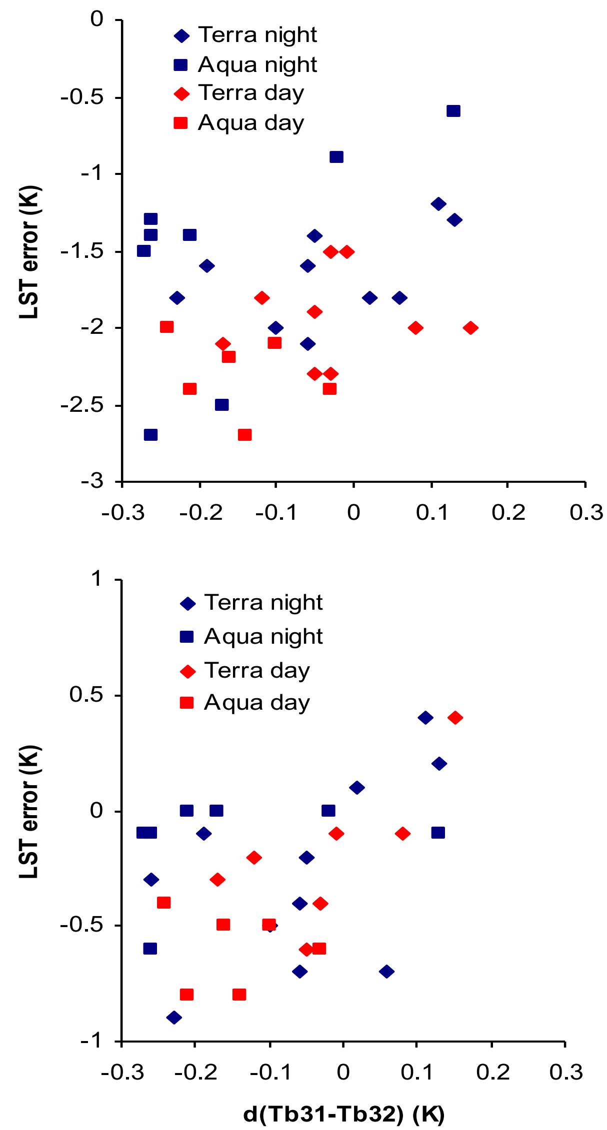

LST errors at site 38 (Tamanrasset) in V5 (upper) and V6 (bottom).

New Improvements for the C6 LST Product (cont.)

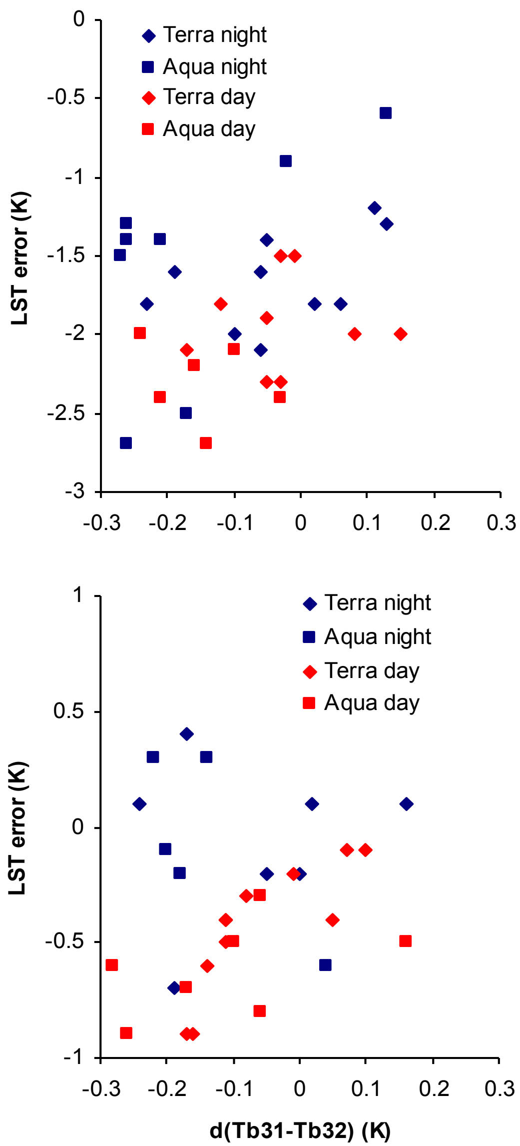

LST errors at site 39 (Bechar) in V5 (upper) and V6 (bottom).

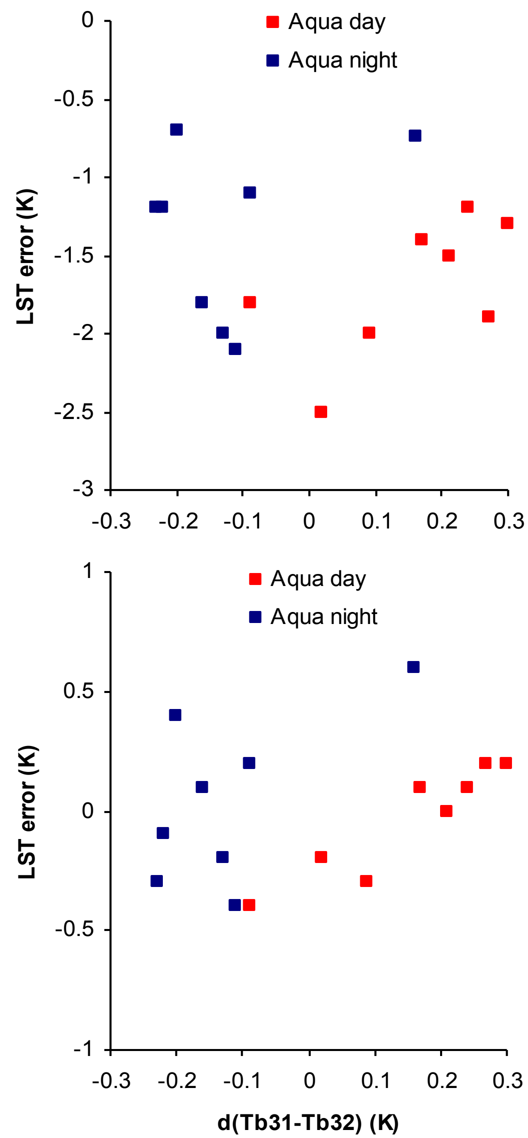

LST errors at site 41 (South of Valley Univ.) in V5 (upper) and V6 (bottom). **NCEP profiles were used in the nighttime cases at this site.**

Comparison between V5 and V6 daytime LSTs at three bare soil sites in North Africa

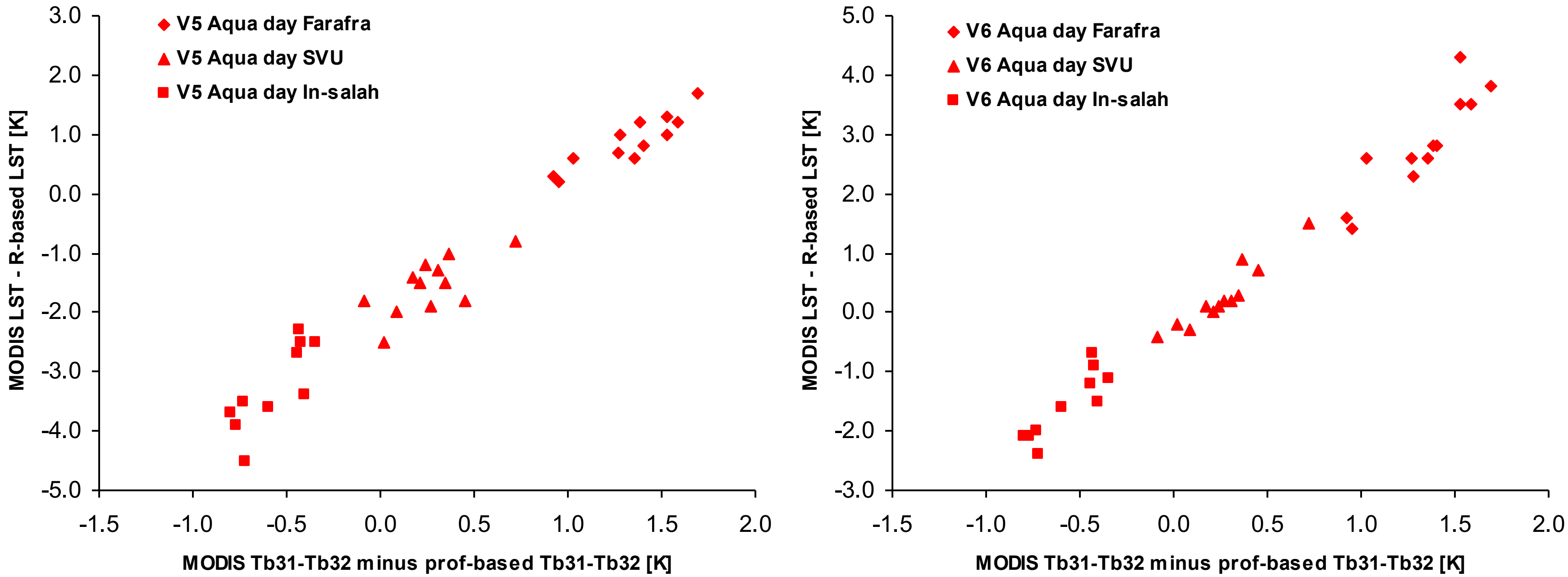

Comparison of errors in daytime Aqua MODIS LSTs at sites 40-42 (Farafra, SVU, and In-salah) in V5 (left) and V6 (right) indicates that V6 LSTs are about 2K higher than V5 LSTs and that the similar linear relation between LST errors and d(Tb31 – Tb32) values is mainly due to the differences in surface emissivities in bands 31 and 32 at the three bare soil sites.

Comparison of C6 LST Product to C5 and C41 (1)

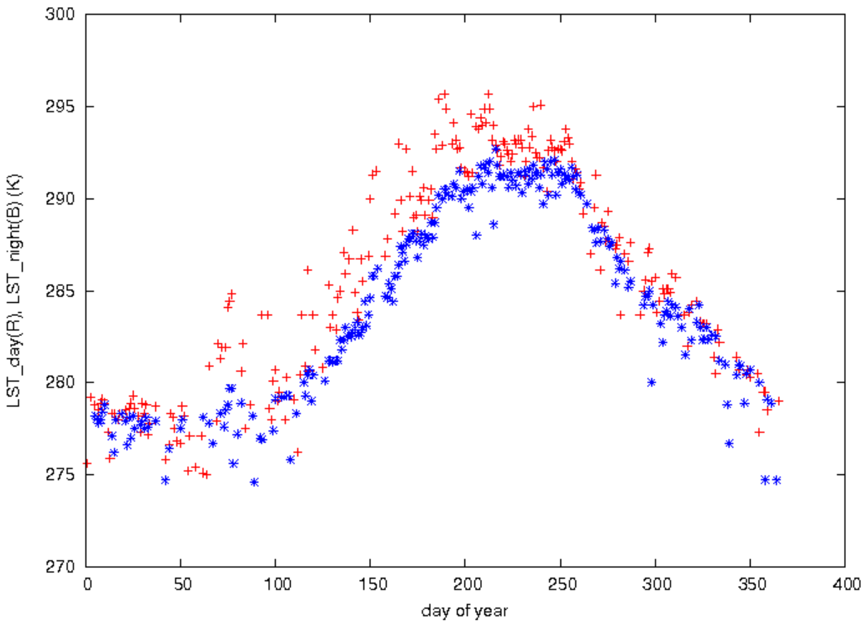

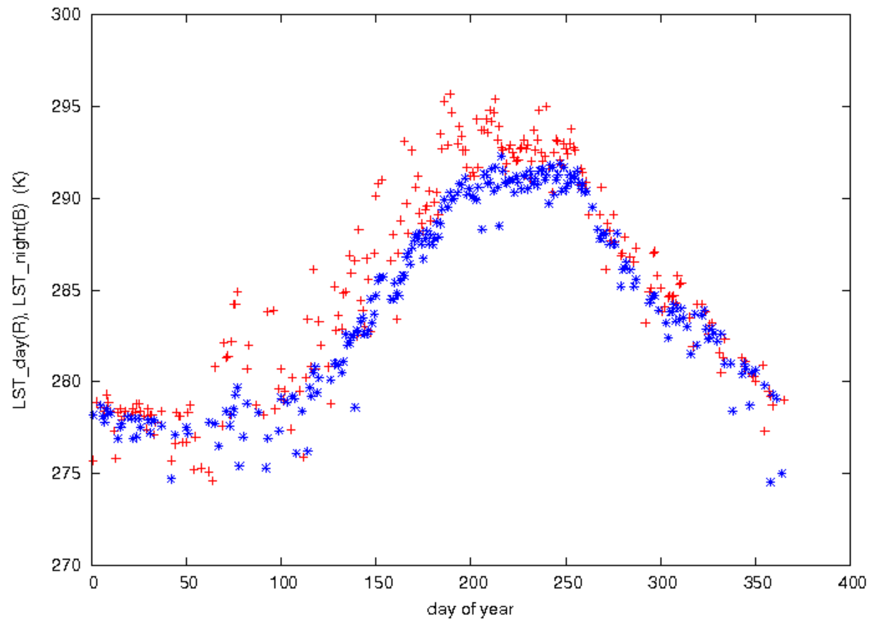

LST_day (red) and LST_night (blue) at Lake Tahoe, CA, retrieved by the day/night algorithm in the MYD11B1 product in 2007 in C6 (above), C5 (upper right) and C41 (lower right).

Note that Lake Tahoe does not freeze in the whole year so the low LST values in the C41 are due to cloud contaminations.

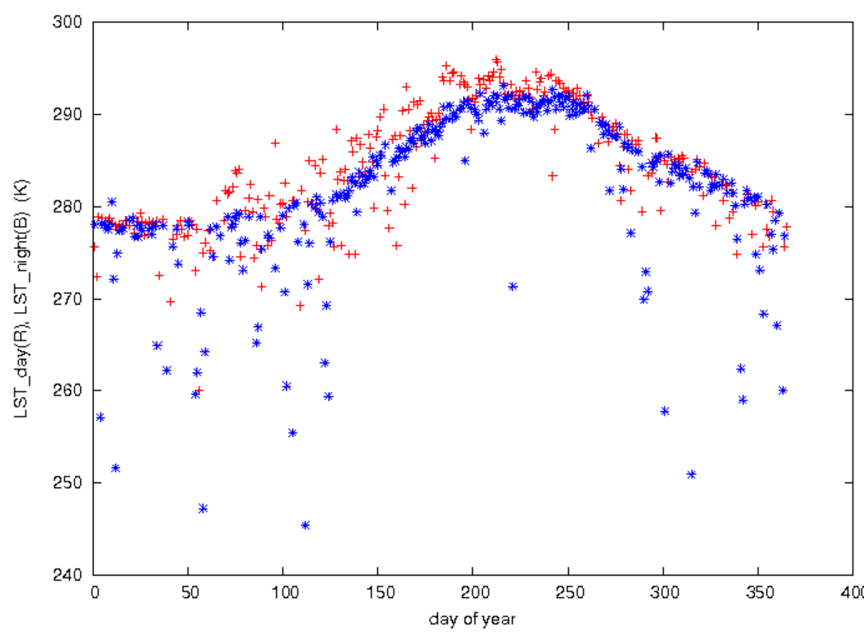

Comparison of C6 LST Product to C5 and C41 (2)

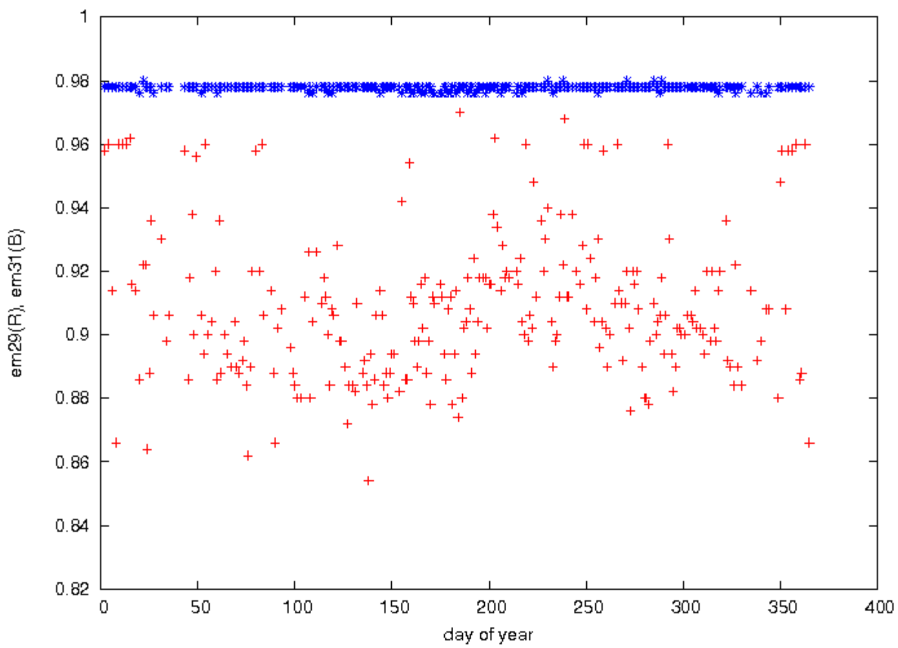

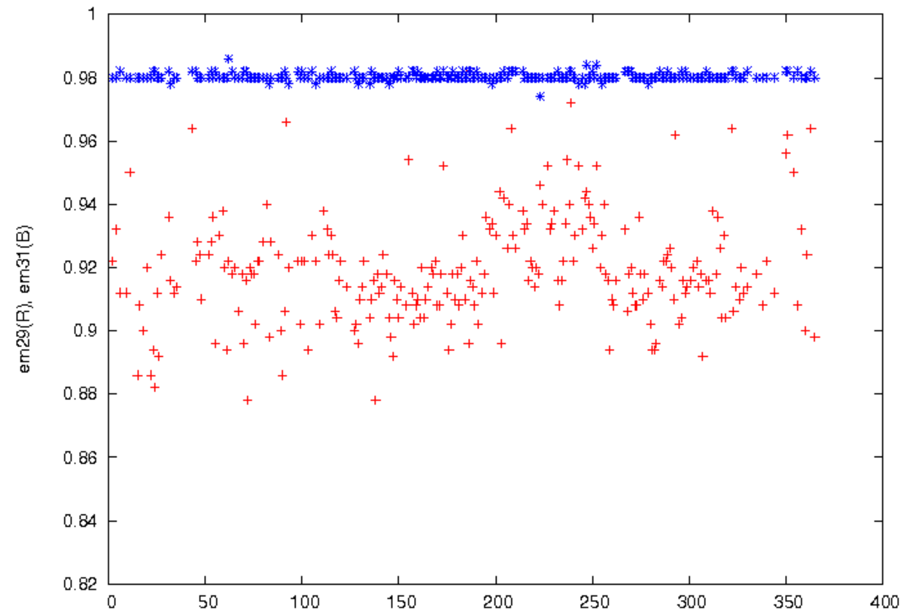

em29 (red) and em31 (blue) at a shrubland in Mojave, CA, retrieved by the day/night algorithm in the MYD11B1 product in 2007 in C6 (above), C5 (upper right) and C41 (lower right).

Many emissivity values in the C41 are too low, which would correspond to unreasonably high LSTs.

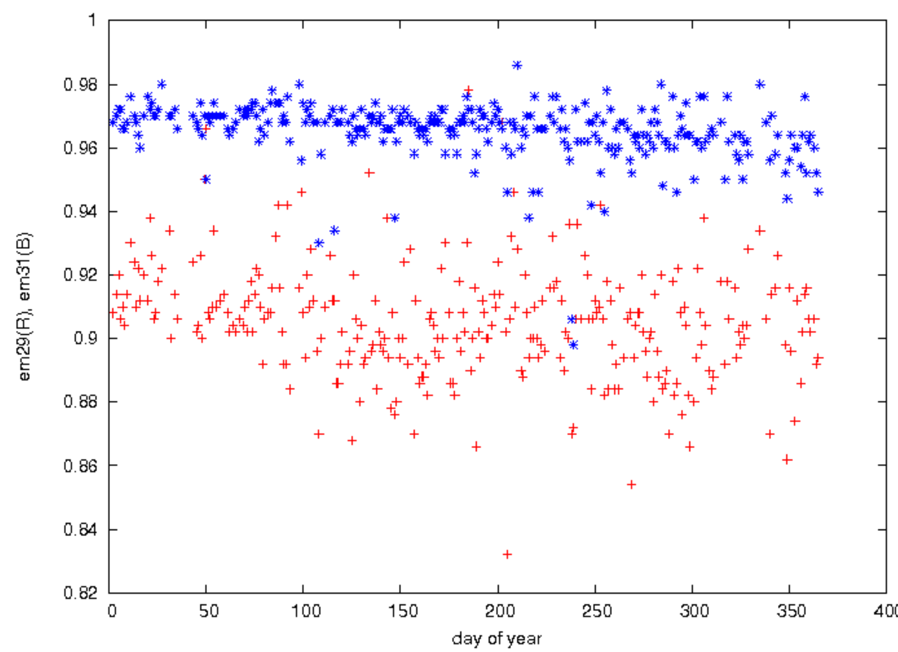

A short list of references

Coll, C., Wan, Z., & Galve, J.M., (2009). Temperature-based and radiance-based validation for the V5 MODIS land-surface temperature product. *JGR,* 114, D20102, doi:10.1029/2009JD012038.

Wan, Z., (2008). New refinements and validation of the MODIS land-surface temperature/emissivity products. *Remote Sensing of Environment*, 112, 59-74.

Wan, Z., & Li, Z.-L., (2008). Radiance-based validation for the V5 MODIS land-surface temperature product. *International Journal of Remote Sensing*, 29, 5373-5395.

Coll, C., Caselles, V., Galve, J.M., Valor, E., Niclòs, R., Sánchez, J.M., & Rivas, R. (2005). Ground measurements for the validation of land surface temperatures derived from AATSR and MODIS data. *Remote Sensing of Environment*, 97, 288-300.

Snyder, W.C., Wan, Z., Zhang, Y., & Feng, Y.-Z. (1998). Classification-based emissivity for land surface temperature measurement from space. *International Journal of Remote Sensing*, 19, 2753-2574.

Wan, Z., & Dozier, J. (1996). A generalized split-window algorithm for retrieving land-surface temperature from space. *IEEE Trans. Geoscience and Remote Sensing,* 34, 892–905.

Wan, Z., & Li, Z.-L. (1997). A physics-based algorithm for retrieving land-surface emissivity and temperature from EOS/MODIS data. *IEEE Trans. Geoscience and Remote Sensing*, 35, 980-996.

Wan, Z., Zhang, Y., Zhang, Y.Q., & Li, Z.-L. (2002). Validation of the land-surface temperature products retrieved from Moderate Resolution Imaging Spectroradiometer data. *Remote Sensing of Environment*, 83, 163-180.

Wan, Z., Zhang, Y., Zhang, Y.Q., & Li, Z.-L. (2004). Quality assessment and validation of the global land surface temperature. *International Journal of Remote Sensing*, 25, 261-274.

http://www.icess.ucsb.edu/modis/LstUsrGuide/usrguide.html